ISBN: 978-3-95450-247-9 ISSN: 2673-5490 doi: 10.18429/JACoW-IPAC2024-THPG11

LONG RANGE PLASMA EXPERIMENT BEAM TRANSPORT WITH UCLA MITHRA BEAMLINE

M.Yadav*, A. Fukasawa, K. Letko, Sean O' Tool, P. Manwani, F. Bosco, G. Lawler, B. Naranjo, J. Phillips, O. Williams, Y. Sakai, G. Andonian, J. B. Rosenzweig
University of California, Los Angeles, CA, USA

Abstract

We present a comprehensive simulation study of the plasma wakefield acceleration (PWFA) interaction using the advanced, fully relativistic, three-dimensional Particle-in-Cell (PIC) code, OSIRIS. Our research aims to develop optimized beam-matching optics to effectively transport the MITHRA beam into the Large Plasma Device (LAPD) to understand long-range plasma effects. Using the beam data generated from the MITHRA hybrid gun, we have performed optimization simulations with the beam dynamics software, elegant.

INTRODUCTION

Megavolt InTense High-gradient Research Accelerator (MITHRA) is a UCLA lab dedicated to advanced accelerator and light source research, developed by the Particle Beam Physics Lab's (PBPL) extensive collaborations. The facility is equipped with a 30 MeV electron beam, terawatt lasers, cryogenic cooling, multiple RF and plasma technologies. It's currently under commissioning, with initial experiments at 30 MeV, moving towards the envisioned 80 MeV setup as shown in Fig. 1. After the installation of 1.5 m linear accelerator (LINAC) at MITHRA, which is set to chieve a beam energy of 30 MeV by late 2024, it will facilitate a diverse array of experiments, including space plasma, dielectric structures, inverse Compton scattering and long range plasmas [1–4].

LAPD is a national user facility in the science and technology building, one floor below MITHRA lab, for creation of very large volume quiescent plasmas with large diagnostic capabilities. LAPD plasmas are generated using a combination of two different LaB_6 hot-cathode sources. The main plasma source uses a relatively large area, circular hot-cathode (38 cm diameter), mounted at one end of the device in a strong magnetic field region ($B_m = 0.9$ T). A small rectangular hot-cathode (size: 20 cm × 20 cm) source is mounted at the opposite end to help augment the density in this region. Primary electrons emitted from these hot-cathodes are accelerated by semitransparent grid anodes, located near the cathodes. The ionizing electrons strike an inert, neutral gas and generate from highly ionized to fully ionized plasmas [5–7]. Highly reproducible, quiescent plasmas are formed, having typical discharge duration of 1-17 ms at a 1 Hz repetition rate. After the discharge pulse is terminated, the electron temperature falls rapidly, but the plasma density remains confined for long times, thus permitting additional access to experimentation in afterglow conditions for intervals exceeding 50 ms. The LAPD plasma column has a maximum length of 21 m and a 75 – cm diameter. The confining magnetic field can achieve a steady-state value of up to 2.5 kG, with an upgrade now being developed to go to 9 kG. The magnetic confining field permits exploration of plasma wave excitation to over $n_0 = 5 \times 10^{13}$ cm^{-3}, even recently demonstrating $n_0 = 8 \times 10^{13}$ cm^{-3} [8].

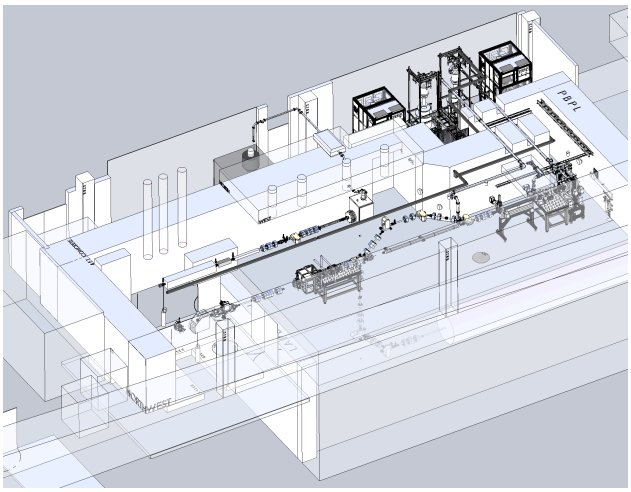

Figure 1: CAD model of the MITHRA laboratory, featuring a bunker, a klystron gallery, and an accelerator. The klystron gallery is equipped with the first 25 MW XK-5 and a modulator. It currently supports a low-energy beamline of approximately 4 MeV, with plans for a 1.5-meter linac upgrade to boost the energy to 30 MeV.

In this paper we propose a long range plasma experiment at MITHRA lab. We discuss the transport possibilities of injecting the MITHRA beam into the LAPD to understand PWFA interactions. We discuss the effects of magnetic fields on the blowout. Finally, conclude with the implications of our research for experiments with intense beams.

PROPOSED EXPERIMENT AT MITHRA

At the LAPD, a considerable variety of plasma diagnostics are available, operating at the repetition rates needed for different experiments. The beam transport line for bringing the high current beams to the LAPD has been introduced. For clarity we show diagram in projection, illustrative the vertical bend systems in Fig. 2. These 90° modular bends are constructed from a double-bend achromat (DBA) approach, where the transverse dispersion is cancelled at the end of the second 45° bend magnets by judicious choice of the

* yadavmonika@physics.ucla.edu

Content from this work may be used under the terms of the CC BY 4.0 licence (© 2024). Any distribution of this work must maintain attribution to the author(s), title of the work, publisher, and DOI.

ISBN: 978-3-95450-247-9 ISSN: 2673-5490 doi: 10.18429/JACoW-IPAC2024-THPG11

Content from this work may be used under the terms of the CC BY 4.0 licence (© 2024). Any distribution of this work must maintain attribution to the author(s), title of the work, publisher, and DOI.

Table 1: Beam Parameters for Different Densities

Parameter	4e13	5e13	8e13
Beam charge	250 pC	250 pC	250 pC
Norm. rms emittance	3.2 mm-mrad	3.2 mm-mrad	3.2 mm-mrad
Energy	30 MeV	30 MeV	30 MeV
beta	7 mm	6.7 mm	5.3 mm
Sigma_x,y	24 µm	23.17 µm	20.57 µm
Sigma_z	100 µm	100 µm	100 µm
Peak density	15	11.82	9.75
Skin Depth	8.4e-4 m	7.51e-4 m	5.94e-4 m

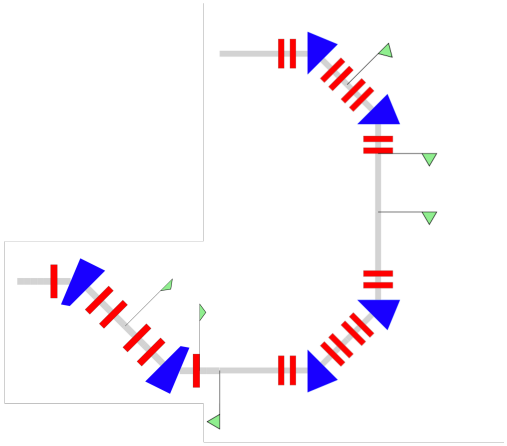

Figure 2: Long range plasma transport from MITHRA lab to LAPD.

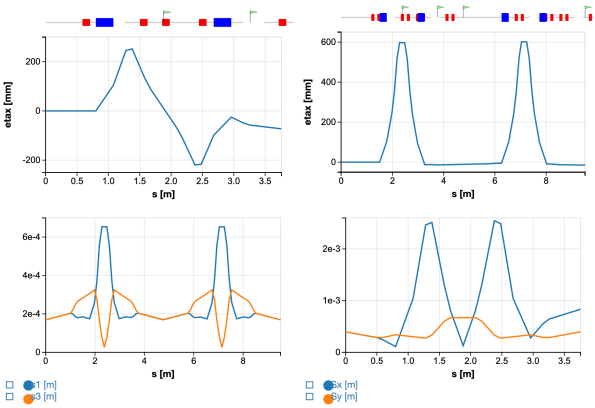

Figure 3: Dispersion is cancelled due to double-bend achromat. Evolution of the standard deviation in x and y for the double bend case.

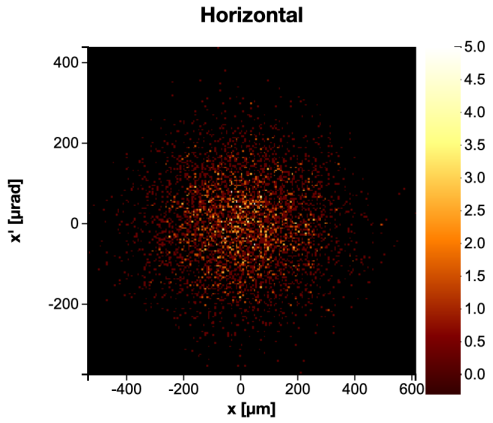

Figure 4: Horizontal beam profile at the end of the LAPD transport.

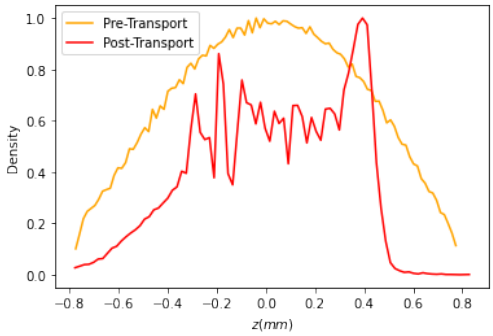

Figure 5: Yellow line is the pre-transport beam profile and red line is the post-transport beam profile.

quadrupole triplet settings. In Fig. 3 dispersion with respect to distance is plotted. In Fig. 4 shows the horizontal beam profile at the end of the LAPD transport.

In Fig. 3, standard deviation with respect to distance is plotted. In Fig. 5, the yellow line is the pre-transport density variation of the beam, and the red line is the post-transport beam profile. The optimized initial conditions for beam transport after acceleration in the 1.5 m linac up to over 30 MeV are shown in Table 1. The beam has over 70 A peak current and a compact longitudinal phase space (1.2 ps rms) with good emittance, $\varepsilon_n \simeq 1-3$ mm-mrad. A simple first order achromatic bend is achieved by splitting the bend equally in two bend magnets and placing a quadrupole between them. This quadrupole cancels dispersion by imaging the center of the first bend magnet onto the center of the second helps preserve the emittance.

A promising scenario has been simulated for the MITHRA case using the PIC code OSIRIS [9], with the achievable charge 250 pC needed to provide enough beam density. This is at the nominal optimal energy that we obtain using the

ISBN: 978-3-95450-247-9 ISSN: 2673-5490 doi: 10.18429/JACoW-IPAC2024-THPG11

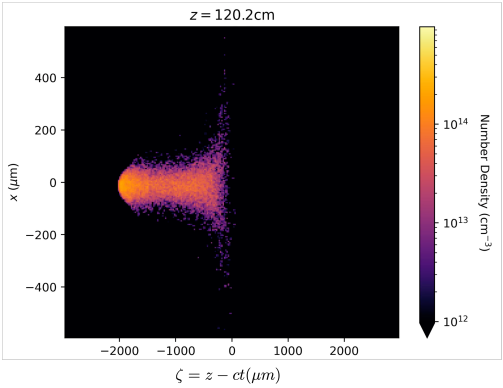

Figure 6: Drive beam propagating in 5e13 /cc plasma density. All the parameters are same as described in Table 1.

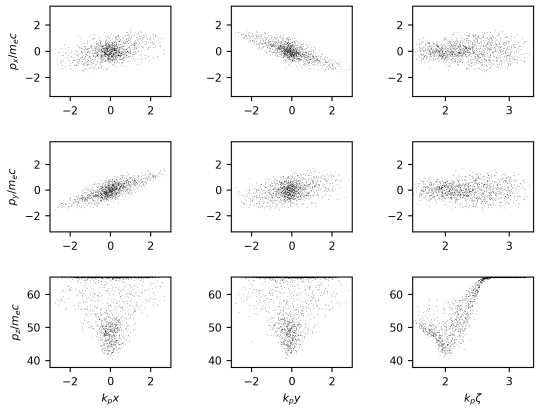

Figure 7: Phase space of the beam, in the case of a long beam the head of the beam oscillates with different frequency with respect to tail of the beam.

1.5 m linac after the photoinjector, as with the LAPD case. The long range beam behaviour is shown in Fig. 6. The beam starts to degrade after 3-4 meters propagation, and the region becomes interesting for the plasma aftereffects. In Fig. 7, the phase space matrix is plotted to show the evolution of the beam and how the energy is being distributed after propagating to a few meters in plasma.

This beam, with $\sigma_z = 95\,\mu$m, is numerically injected into a $n_0 = 10^{13}$ cm^{-3} plasma, yielding the condition with $k_p\sigma_z \simeq 2$. The head of the beam is decelerated while the tail is accelerated, thus producing the desired distribution as shown in the phase space plot in Fig. 7. The ion focusing in this case is very strong, resulting in a matched transverse beam size of $\sigma_x \simeq 5\,\mu$m. This beta-matching is obtained by using a strong, adjustable permanent magnet quadrupole triplet. The matching process is completed by utilizing the up-ramp of the plasma density that increases the focusing strength. At the LAPD, introduction of a highly magnetized plasma yields yet another variable that can give a very strong effect on the system's long-term behavior. The initiation of the interaction is shown in Fig 8, which shows, in the very short

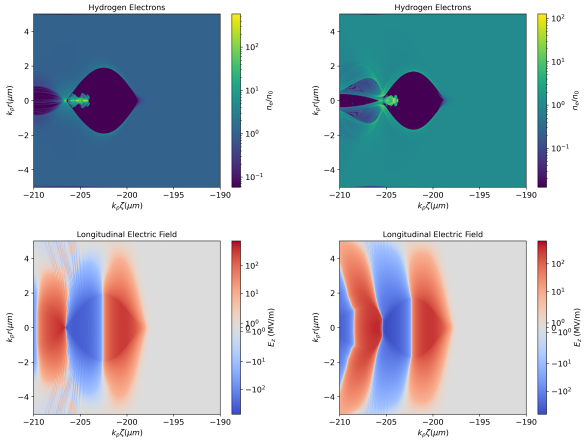

Figure 8: Comparison of no magnetic field and magnetic field for a beam propagating in plasma.

term, plasma wavelength-scale response to the beam's wake excitation. Most critically, we show the differences between the unmagnetized and the highly-magnetized cases. In the magnetized (0.9 T) scenario, one avoids nearly completely the density spikes at the end of the blowout bubble. Efforts are currently underway to finalize the beam transport system to the LAPD.

CONCLUSION

An improved generation of dipole magnets is currently under design at the PBPL, needed for LAPD and other beamlines at MITHRA Lab. It may be necessary to preserve both transverse and longitudinal phase space qualities to introduce sextupoles near the first and last quadruples in the triplets, to correct second-order effects that prove damaging to the beam. It may be necessary to complete the transport with a small chicane to tune the longitudinal focusing after the bends. In this study, we thoroughly examined the transport and optimization of the MITHRA beamline for use in PWFA experiments at the LAPD. We did initial optimization for the beam-matching conditions necessary to efficiently inject the beam from the MITHRA lab's low-energy setup into the LAPD's plasma environment. The use of magnetized and non-magnetized plasma settings provided valuable insights into the impact of external magnetic fields on beam dynamics and plasma behavior. This understanding is crucial for control on the size of the blowout for a better injection of the witness beam.

ACKNOWLEDGEMENT

This work was performed with the support of the US Department of Energy, Division of High Energy Physics, under Contract No. DE-SC0009914, DE-SC0017648, NSF PHY-1549132 Center from Bright Beams, DARPA under Contract N.HR001120C007.

Content from this work may be used under the terms of the CC BY 4.0 licence (© 2024). Any distribution of this work must maintain attribution to the author(s), title of the work, publisher, and DOI.

ISBN: 978-3-95450-247-9 ISSN: 2673-5490 doi: 10.18429/JACoW-IPAC2024-THPG11

© Content from this work may be used under the terms of the CC BY 4.0 licence (© 2024). Any distribution of this work must maintain attribution to the author(s), title of the work, publisher, and DOI.

REFERENCES

[1] A. Fukasawa *et al.*, "Progress on the hybrid gun project at ucla," *Physics Procedia*, vol. 52, pp. 2–6, 2014. doi:10.1016/j.phpro.2014.06.002

[2] G. E. Lawler *et al.*, "Cyborg Beamline Development Updates," in *Proc. NAPAC'22*, Albuquerque, NM, USA, 2022, pp. 512–515. doi:10.18429/JACoW-NAPAC2022-TUPA80

[3] J. Rosenzweig *et al.*, "Design and applications of an x-band hybrid photoinjector," *Nucl. Instrum. Methods Phys. Res., Sect. A*, vol. 657, no. 1, pp. 107–113, 2011, X-Band Structures, Beam Dynamics and Sources Workshop (XB-10). doi:10.1016/j.nima.2011.05.046

[4] J. Rosenzweig *et al.*, "Ultra-high brightness electron beams from very-high field cryogenic radiofrequency photocathode sources," *Nucl. Instrum. Methods Phys. Res., Sect. A*, vol. 909, pp. 224–228, 2018. doi:10.1016/j.nima.2018.01.061

[5] W. Gekelman *et al.*, "The upgraded Large Plasma Device, a machine for studying frontier basic plasma physics," *Rev. Sci. Instrum.*, vol. 87, no. 2, 2016, 025105. doi:10.1063/1.4941079

[6] D. T. Palmer *et al.*, "Emittance Studies of the BNL/SLAC/UCLA 1.6 Cell Photocathode RF Gun," in *Proc. PAC'97*, Vancouver, Canada, May 1997, pp. 2687–2689. doi:10.1109/PAC.1997.752732

[7] M. Yadav *et al.*, "Studying the basics of plasma physics using long range plasma," 2023.

[8] B. Spataro *et al.*, "Rf properties of a x-band hybrid photoinjector," *Nucl. Instrum. Methods Phys. Res., Sect. A*, vol. 657, no. 1, pp. 99–106, 2011. doi:10.1016/j.nima.2011.04.057

[9] R. Fonseca *et al.*, "Osiris: A three-dimensional, fully relativistic particle in cell code for modeling plasma based accelerators," 2002, pp. 342–351. doi:10.1007/3-540-47789-6_36